HHS Public Access

Author manuscript

Cancer Res. Author manuscript; available in PMC 2020 December 15.

Published in final edited form as:

Cancer Res. 2020 June 15; 80(12): 2663–2675. doi:10.1158/0008-5472.CAN-19-3068.

Telomere Maintenance Mechanisms Define Clinical Outcome in High-Risk Neuroblastoma

Balakrishna Koneru[1,2], **Gonzalo Lopez**[3,4], **Ahsan Farooqi**[1,2], **Karina L. Conkrite**[3,4], **Thinh H. Nguyen**[1], **Shawn J. Macha**[1,2], **Apexa Modi**[3,4], **Jo Lynne Rokita**[3,4,5], **Eduardo Urias**[1], **Ashly Hindle**[1,2], **Heather Davidson**[1], **Kristyn Mccoy**[1], **Jonas Nance**[1], **Vanda Yazdani**[1], **Meredith S. Irwin**[7], **Shengping Yang**[1], **David A. Wheeler**[6], **John M. Maris**[3], **Sharon J. Diskin**[3,4], **C. Patrick Reynolds**[1,2,*]

[1]Cancer Center and Department of Pediatrics, School of Medicine, Texas Tech University Health Sciences Center School of Medicine, Lubbock, TX, USA

[2]Department of Cell Biology and Biochemistry, Texas Tech University Health Sciences Center, Lubbock, TX, USA

[3]Division of Oncology, Children's Hospital of Philadelphia and Perelman School of Medicine at the University of Pennsylvania, Philadelphia, PA, 19104-4318, USA

[4]Department of Bioinformatics and Health Informatics, Children's Hospital of Philadelphia, Philadelphia, PA, 19104, USA

[5]Center for Data-Driven Discovery in Biomedicine, Children's Hospital of Philadelphia, Philadelphia, PA, 19104, USA

[6]Human Genome Sequencing Center, Baylor College of Medicine, Houston, TX, 77030, USA

[7]Department of Pediatrics, The Hospital for Sick Children, Toronto, ON, Canada

Abstract

Neuroblastoma is a childhood cancer with heterogeneous clinical outcomes. To comprehensively assess the impact of telomere maintenance mechanism (TMM) on clinical outcomes in high-risk neuroblastoma, we integrated the C-circle assay (a marker for alternative lengthening of telomeres (ALT)), TERT mRNA expression by RNA sequencing, whole genome/exome sequencing, and clinical co-variates in 134 neuroblastoma patient samples at diagnosis. In addition, we assessed TMM in neuroblastoma cell lines (n=104) and PDX (n=28). ALT was identified in 23.4% of high-risk neuroblastoma tumors and genomic alterations in ATRX were detected in 60% of ALT tumors; 40% of ALT tumors lacked genomic alterations in known ALT-associated genes. High-risk neuroblastoma patients were classified into 3 subgroups (TERT-high, ALT+, and TERT-low/non-ALT) based on presence of C-circles and TERT mRNA expression (above or below median TERT expression). Event-free survival was similar among TERT-high, ALT+, or TERT-low/non-ALT patients. However, overall survival (OS) for TERT-low/non-ALT patients was significantly higher relative to TERT-high or ALT patients (log-rank test; $P < 0.01$) independent of current clinical and

[*]**Correspondence:** C. Patrick Reynolds, MD PhD, **Address:** Cancer Center, Texas Tech University Health Sciences Center School of Medicine, 3601 4th Street, Mail Stop 9445, Lubbock, Texas 79430-6450, **Phone:** 806-743-1558, patrick.reynolds@ttuhsc.edu.

Conflicts of interest statement: The authors declare no potential conflicts of interest

molecular prognostic markers. Consistent with the observed higher OS in patients with TERT-low/non-ALT tumors, continuous shortening of telomeres and decreasing viability occurred in low TERT-expressing, non-ALT patient-derived high-risk neuroblastoma cell lines. These findings demonstrate that assaying TMM with TERT mRNA expression and C-circles provides precise stratification of high-risk neuroblastoma into three subgroups with substantially different OS: a previously undescribed TERT-low/non-ALT cohort with superior overall survival (even after relapse) and two cohorts of patients with poor survival that have distinct molecular therapeutic targets.

Keywords

ALT; TERT; Neuroblastoma; High-risk; Clinical-outcomes

Introduction

Unlimited proliferation of cancer cells requires that they maintain telomeres (1), which are typically maintained by activating telomerase (2). *TERT* encodes the catalytic component of telomerase (3,4). Cancer cells activate telomerase by acquiring *TERT* promoter mutations, *TERT* genomic alterations, or transcriptional dysregulation (5–8). *TERT* mRNA levels correlate with telomerase activity (9,10) and is often used to infer telomerase activity in cancer (5,9–11). Some cancers do not express *TERT* mRNA and use the recombination-mediated alternative lengthening of telomeres (ALT) mechanism (12). Telomeric repeats in the form of partially double-stranded DNA, termed C-circles, provide a highly specific marker for ALT activity (13). ALT is commonly associated with loss-of-function genomic alterations in *ATRX* or its binding partner *DAXX* (14–16), and less commonly with mutations in *H3F3A* (17) or *SMARCAL1* (18).

Neuroblastoma is a malignant childhood cancer arising from the developing sympathetic nervous system with clinical behavior that ranges from spontaneous regression to relentless and fatal tumor progression in spite of multimodal intensive therapy (19). High-risk neuroblastoma, as defined by stage, age, histology, and *MYCN* genomic amplification, has an overall survival rate ~ 50% with current intensive therapy (20–22). In addition to known oncogenic drivers, including *MYCN* amplification and *ALK* mutations (23,24), recent whole genome and exome sequencing studies demonstrated structural rearrangements near the *TERT* locus in ~25% of high-risk neuroblastomas (5,11) and largescale structural variations (SVs) in the chromatin remodeler gene *ATRX* in ~10% of high-risk neuroblastomas (24).

Of these four most frequent genomic alterations identified in neuroblastomas, three converge on activating telomere maintenance mechanisms (TMMs) (5,24). Tumors with *MYCN* amplification or *TERT* rearrangements activate telomerase by inducing *TERT* mRNA expression (5,11), while loss of *ATRX* is implicated in the ALT phenotype (14–16). Genomic amplification of *MYCN, TERT* genomic rearrangements, and loss of *ATRX* are nearly always mutually exclusive events, suggesting a functional redundancy between these mechanistic pathways. Telomere maintenance has long been thought to be pivotal for high-risk neuroblastoma (25). However, neuroblastoma cell lines with high telomere content and

continually shortening telomeres due to lack of a TMM (termed the ever-shorter telomere (EST) phenotype) have been described and analysis of primary patient tumors suggested that EST comprises >10% of high-risk patient tumors (26).

A recent study of TMM in neuroblastoma reported that 3% of high-risk neuroblastoma tumors lacked evidence of TMM activation (27), but that study employed *TERT* expression by microarray and defined ALT by detecting ALT-associated promyelocytic leukemia bodies (APBs). Unlike the specific and sensitive C-circle assay (13), APBs can also be detected in non-ALT cells with long telomeres due to an increased frequency of telomere trimming events (28). Thus, the true frequency and clinical relevance of TMM-negative (EST phenotype) tumors in high-risk neuroblastoma remains to be defined.

To comprehensively define TMMs and their clinical impact in high-risk neuroblastoma, we employed the ALT-specific C-circle assay, telomere content measurement by qPCR, and *TERT* mRNA expression measurement by RNA sequencing in 134 neuroblastoma primary tumors (110 high-risk and 24 non-high-risk). Genomic sequencing data for most of these tumors was available from the National Cancer Institute TARGET program (https://ocg.cancer.gov/programs/target;accession#phs000467) and was integrated with clinical risk stratification and outcome data. We also assessed *TERT* expression, C-circles, telomere content in patient-derived cell lines (n=103) and xenografts (n=28) established from high-risk neuroblastomas.

Materials and Methods

Patient Samples and Clinical Data

Primary tumor samples prior to therapy were collected (snap-frozen) with written informed consent from children with neuroblastoma entered on to Children's Oncology Group protocols. Pilot sections of tumors verified tumor content. RNA and DNA were extracted, RNA quality monitored by RIN values, and subjected to RNA and DNA sequencing by the NCI TARGET program (24). DNA and RNA were provided to TTUHSC for C-circle, telomere content, and RT-PCR for *TERT* mRNA expression.

Analysis of *TERT* and *ATRX* Structural Variants

Structural variations from whole genomes (CGI) used a combination of alignment based and read-depth based approaches. Alignment based SVs are initially obtained through The CGI Cancer Pipeline 2.0. Read-depth breakpoints were obtained from segmentation profiles generated from tumor/blood matched log R ratios from every 2Kb window across the genome; *ATRX* variants were as previously described for the WES dataset (24,29).

C-circle and Telomere Content Assay

C-circle assay (13), amplified C-circles, detected using telomere qPCR or slot-blotting, (26,30) and telomere content assay by qPCR (26) were performed as previously described.

TERT Expression and Telomeric Repeat Amplification Protocol (TRAP) Assay

TERT mRNA expression was measured by RNA sequencing, validated by RT-PCR, details in supplementary methods. TRAP assay was performed on whole cell lysate from selected cell lines and PDXs using either TRAPeze Telomerase Detection kit (EMD Millipore) or TeloTAGGG Telomerase PCR ELISA kit (Roche) as previously described (31).

Terminal Restriction Fragment (TRF) Analysis

TRF analysis was performed as previously described (32).

Expression Plasmids

For constitutive overexpression, *MYCN* was cloned into pLenti-C-Myc-DDK-IRES-Puro (Origene; PS100069).

Cell Lines and Patient-Derived Xenografts

All neuroblastoma patient-derived cell lines and patient-derived xenografts (PDXs) were obtained from the ALSF/Children's Oncology Group (COG) Childhood Cancer Repository at Texas Tech University Health Sciences Center (www.CCcells.org). All cell line and PDX identities were confirmed using the AmpFLSTR Identifier Plus PCR Amplification kit (Applied Biosystems) at time of use for experimentation, verified against the STR database at www.CCCells.org. Neuroblastoma cell lines were used at passage numbers below 25, except when noted in results, were cultured in antibiotic-free medium, and routinely tested for lack of mycoplasma contamination. A total of 28 neuroblastoma PDXs were used in this study all employed at passage 2 in mice. PDXs were all verified to be free of human pathogens and Epstein-Barr virus by PCR.

Statistics

R (Version 3.3.2), SAS software (SAS Institute, Cary, NC, USA), IBM SPSS (V25) and GraphPad Prism (version 7.0a) were used for statistical analysis and data representation. Differences in *TERT* mRNA expression, telomere content, and telomerase activity between subgroups used the Wilcoxon rank-sum test. Associations of phenotype with clinical risk factors used Fisher's exact test. Survival comparisons were by the Kaplan-Meier log-rank method using the R "survival" package (http://cran.r-project.org/web/packages/survival/index.html). Event-free survival (EFS) was calculated as time from initial diagnosis to the first occurrence of either relapse, progressive disease, secondary malignancy or death. Patients without events were censored at the time of last follow-up. Overall survival (OS) was defined as time from initial diagnosis until time of death from any cause, alive patients censored at last contact. Multivariate Cox regression was used to estimate the prognostic impact of *TERT* mRNA expression and C-circle presence while adjusting for *ALK* alterations, *RAS/P53* alterations, ploidy, *MYCN* amplification, and *11q* chromosome arm loss for both EFS and OS. Age and stage of the patients were not included in the final model, as all the patients in survival analysis were stage 4 high-risk patients with age at diagnosis > 18 months.

See supplementary methods for additional details.

Results

Patient Characteristics and Integrated Resources

To comprehensively assess telomere maintenance mechanisms and their clinical relevance in high-risk neuroblastoma, we integrated the C-circle assay (n=145), telomere content assay (n=145), RNA sequencing (RNA-seq; n=160), whole genome sequencing (WGS; n=136), whole exome sequencing (WES; n=222), and clinical co-variates (data availability and overlap is presented in Supplementary Fig. S1). All specimens were obtained at initial diagnosis with written informed consent at Children's Oncology Group member institutions in accordance with recognized ethical guidelines (24). Most cases assessed in this study are stage 4 high-risk neuroblastoma patients over 18 months of age (n = 107), with 3 < 18-month-old high-risk patients and 24 patients being classified as low- or intermediate-risk. All samples analyzed had > 70% tumor content on pilot sections and high-quality nucleic acids.

Alternative Lengthening of Telomeres (ALT) and *ATRX* Genomic Alterations in Neuroblastoma

To investigate the prevalence of ALT in neuroblastoma, we quantified C-circles by qPCR for 134 primary tumors (110 high-risk (30 *MYCN*-amplified), 12 intermediate-risk, and 12 low-risk) selected solely based on DNA availability (Table 1; Supplementary Table S1). Of the 107 high-risk tumors (age > 18 months), 25 (23.4%; 95% CI: 15.3–31.4%) were positive for the ALT biomarker C-circles (Fig. 1A; Supplementary Table S1). For 23 of 25 ALT tumors WGS and/or WES data was available; *ATRX* genomic alterations were observed in 13 of 23 ALT tumors (57%) (10 focal deletions, 2 missense and 1 nonsense mutations; Table S1); 9 focal deletions and the 3 single nucleotide variants (SNVs) were previously reported (24), while one sample with an *ATRX* focal deletion (PATCFL) was missed in the previous WES study (Supplementary Fig. S2A) (24). None of the non-ALT tumors (C-circle negative) with WGS and/or WES (n=102) had *ATRX* genomic alterations. We assessed C-circles in 11 additional tumor samples previously reported to have *ATRX* genomic alterations including one sample (PASAJU) with a focal gain, and all of them were positive for C-circles (Supplementary Table S1) (24).

Given that *ATRX* deletions commonly appear as intragenic in-frame fusions (15,33), we next explored the effect of *ATRX* variants on transcript levels using String Tie *de novo* assembly and quantification from RNA-seq and 42 different *ATRX* transcripts were predicted; we classified those transcripts into coding, likely coding, non-coding, exonic loss and in-frame fusion (IFF) (Supplementary Fig. S2B). Notably, aberrant transcripts matching IFFs were confirmed as the most expressed isoform in 7 of 10 *ATRX* structural variant ($ATRX^{SV+}$) samples (PATGLU, PAPKXS, PANZVU, PANLET, PARACS, PATCFL, PASTCN and PANLET) while the 3 remaining (PARYNK, PAPKXS and PASRFS) expressed *ATRX* isoforms at very low levels (Supplementary Fig. S2C).

In order to identify additional *ATRX*-altered cases that were missed or not overlapping with the WGS/WES dataset, we compared the total expression of IFF-*ATRX* isoforms against *ATRX*-coding isoforms (Supplementary Fig. S2C). Two additional cases (PAIFXV and

PANBJH) showed overexpression of IFF-*ATRX*, and both cases were positive for C-circles. Considering the combined DNA and RNA variant detection approaches, 10 ALT cases had focal deletions in *ATRX,* 2 cases had higher expression of IFF-like transcripts, and 3 had SNVs (Supplementary Table S1; Fig. 1A and Supplementary Fig. S3). A total of 10/25 ALT tumors had no *ATRX* genomic alterations (Supplementary Table S1; Fig. 1A), which we validated as wild-type for *ATRX* using sanger sequencing. We did not detect genomic alterations in the other known ALT-associated genes (*DAXX*, *H3F3A* or *SMARCAL1*) in *ATRX* wild-type ALT tumors (14,17,18). Event-free survival (EFS) and overall survival (OS) were similar among ALT tumors based on *ATRX* status (Log-rank test; EFS, $P = 0.741$; OS, $P = 0.346$; Supplementary Fig. S4A and S4B).

To further validate activation of ALT in neuroblastoma without *ATRX* genomic alterations, we screened 104 neuroblastoma patient-derived cell lines and 28 neuroblastoma patient-derived xenografts (PDXs) for C-circles using qPCR (Supplementary Table S2); 5 cell lines and 3 PDXs were C-circle positive. C-circle positivity was further confirmed by slot blotting of C-circle assay products onto a nylon membrane, detected using a DIG-labeled telomere probe (Supplementary Fig. S5A). ALT-associated promyelocytic leukemia bodies (APB's) were also observed in ALT cell lines and PDXs (Supplementary Fig. S5B) (34). The ALT cell line SK-N-FI was previously shown to be wild-type for *ATRX* (26,35), and we identified 2 ALT PDXs (COG-N-589x, and COG-N-620x) that were *ATRX* wild-type (Supplementary Fig. S5C) (36). These *ATRX* wild-type ALT cell lines and PDXs were confirmed to express ATRX protein (Supplementary Fig. S5D and S5E). Additionally, none of the *ATRX* wild-type ALT models had mutations in *DAXX*, *H3F3A,* or *SMARCAL1.* Thus, ALT can occur in neuroblastoma with and without *ATRX* genomic alterations.

ALT tumors were significantly associated with later disease onset (Supplementary Fig. S6A). Somatic mutation burden was significantly increased with patient age (Supplementary Fig. S6B) and in ALT tumors (Supplementary Fig. S6C). Consistent with prior reports, ALT tumors were exclusively non-*MYCN*-amplified (non-*MYCN*-Amp) (Fig. 1A; Supplementary Table S3) (35,37), and these cases uniformly showed significantly lower *MYCN* mRNA expression (Fig. S6D). Among the ALT cell lines and PDXs, two ALT cell lines had *MYCN* amplification (copy number assay by qPCR; 32 copies for COG-N-515 and 33 copies for COG-N-512), but *MYCN* mRNA expression in these *MYCN*-Amp ALT cell lines was lower than other non-ALT *MYCN*-Amp cell lines (Supplementary Fig. S6D). We did not find any associations between ALT and segmental chromosomal alterations, regardless of *ATRX* status (Fig. 1A). Frequency of *ALK*, *RAS/MAPK*, and *TP53/CDKN2A* genomic alterations were also similar among ALT and non-ALT tumors (Fig. 1A).

In summary, ~23% of high-risk neuroblastoma tumors are ALT+. ALT activation can occur with and without *ATRX* alterations in neuroblastoma. ALT activation was detected exclusively in non-*MYCN* amplified tumors and in relatively older patients.

TERT Activation in High-risk Neuroblastoma

As it is known that telomerase can be activated by *TERT* genomic rearrangements in neuroblastoma (5,11), we analyzed recurrent SVs affecting the *TERT* locus in 85 neuroblastoma samples that had overlapping WGS, C-circle, and *TERT* expression data

(Fig. 1B). Of 59 high-risk tumors (age > 18 months), 12 (20.3%; 95% CI: 10.1–30.6%) harbored structural rearrangements near the *TERT* gene (Table S1; Fig. 1A), which is consistent with previous reports (5,11). Additionally, as reported previously (29), none of the tumors with WGS had *TERT* promoter mutations..

TERT expression quantified by RNA-seq versus qRT-PCR was strongly correlated in 19 primary tumors (Supplementary Fig. S7A; Spearman Rho = 0.72; $P = 7.83\times10^{-4}$). We assessed whether *TERT* mRNA expression could be used as an alternative to telomerase activity by using neuroblastoma cell lines for which *TERT* expression (by both qRT-PCR and RNA-seq) and telomerase activity (qTRAP by PCR ELISA) were simultaneously quantified (Supplementary Fig. S7B). *TERT* expression by RNA-seq strongly correlated with expression by qRT-PCR (n=23; Supplementary Fig. S7C; Spearman Rho = 0.92; $P = 2.57\times10^{-10}$) and with telomerase enzymatic activity (n=22; Supplementary Fig. S7D; Spearman Rho = 0.95; $P = 6.226\times10^{-12}$). Thus, RNA-seq can reliably quantify *TERT* mRNA expression and is indicative of telomerase activity.

As expected, *TERT* structural variants ($TERT^{SV+}$) tumors had the highest *TERT* mRNA expression, followed by *MYCN*-Amp tumors (Fig. 1C). ALT tumors expressed the least *TERT* of the high-risk subsets (Fig. 1A and 1C). Similar to patient tumors, ALT neuroblastoma cell lines and PDXs had low *TERT* expression (Supplementary Table S2) and were negative for telomerase activity (Supplementary Fig. S8A and S8B). The majority of high-risk tumors without $TERT^{SV+}$, *MYCN* amplification, or ALT had lower *TERT* expression when compared to *MYCN*-Amp or $TERT^{SV+}$ tumors (Wilcoxon $P = 7.6\times10^{-4}$ Fig. 1C), however some had *TERT* expression as high as $TERT^{SV+}$ tumors (Fig. 1C) suggesting the existence of unidentified mechanisms for activation of *TERT* in high-risk neuroblastoma. In our cohort, none of the 24 non-high-risk tumors had high *TERT* expression (Fig. 1C).

Surprisingly, some *MYCN*-Amp tumors had *TERT* expression as low as seen in ALT tumors (Fig. 1C and Supplementary Fig. S9A). These *MYCN*-Amp samples had low *TERT* expression despite having high *MYCN* mRNA expression (Supplementary Fig. S9A). Similar to primary tumors, four *MYCN*-Amp cell lines had low *TERT* expression and were negative for telomerase activity (Table S2; Supplementary Fig. S8B). Knockdown of MYCN expression using *MYCN* shRNA in a *MYCN*-Amp neuroblastoma cell line (COG-N-452h) induced downregulation of *TERT* compared to non-targeted shRNA controls (Supplementary Fig. S9B; $P < 0.05$). Forced overexpression of MYCN using a lentiviral vector was undertaken in four non-*MYCN*-Amp neuroblastoma cell lines: two with telomerase activity (CHLA-171 and Felix-h) and two without telomerase activity (LA-N-6 and CHLA-132, Supplementary Fig. S9C). Forced *MYCN* overexpression upregulated *TERT* expression in one non-*MYCN*-Amp telomerase+ cell line (CHLA-171), but failed to enhance *TERT* expression in the telomerase-positive cell line with a *TERT*-rearrangement (Felix-h), or in the 2 cell lines negative for telomerase activity (Supplementary Fig. S9D, $P < 0.005$). This suggests that MYCN can upregulate *TERT* expression via an intact and non-repressed *TERT* promoter, but MYCN overexpression by itself is not sufficient to overcome the *TERT* repression in *TERT* non-expressing cells.

In summary, *TERT*$^{SV+}$ tumors, and the majority of *MYCN*-Amp tumors had high *TERT* mRNA expression. Some *TERT*^{wt} and *MYCN*^{wt} tumors had *TERT* expression as high as tumors with *TERT*$^{SV+}$, indicating some other unidentified mechanisms for activation of TERT in neuroblastoma. Not all *MYCN*-Amp tumors had high *TERT* expression. Consistent with that observation, forced overexpression of *MYCN* in telomerase-negative cell lines did not induce *TERT* expression.

TERT Expression and ALT Status Predict Poor Outcome in High-risk Neuroblastoma

We analyzed the outcome of 107 stage 4 high-risk patients with age at diagnosis > 18 months for which both *TERT* expression and ALT status were simultaneously assessed (Table S1). High *TERT* expression, defined as ≥ the median *TERT* expression of the high-risk cohort (n=107), was associated with poor overall survival (OS) ($P < 0.001$; Fig. 2A) and poor event-free survival (EFS) ($P = 0.034$; Supplementary Fig. S10A). The 5-year OS was 28% for the *TERT* high (TERT-H) group vs 62% for the *TERT* low (TERT-L) group. However, patients with ALT+ tumors showed no difference from non-ALT patients in OS ($P = 0.99$; Fig. 2B) or EFS ($P = 0.32$; Supplementary Fig. S10B).

Because the OS curves based on ALT status intersect, we computed the Cox regression hazard ratios using time interaction term, and we observed a substantial increase in hazard ratio after 5 years for the ALT group (HR at >5 years: 14.1; $P = 0.024$). In non-ALT tumors, overall survival of high-risk patients was *TERT* expression-dependent, poor with higher *TERT* expression (Supplementary Fig. S11A and S11B). As ALT tumors are a subgroup of TERT-L tumors (all ALT tumors had *TERT* mRNA expression below the median; Supplementary Fig. S9A), we combined analysis of ALT with *TERT* expression, which allowed us to define three groups of patients (TERT-H, ALT, and TERT-L/non-ALT) that each showed distinct OS probabilities (log-rank test comparing three groups, $P < 0.001$; Fig. 2C). The 5-year OS for TERT-H patients was 28% vs 46% for ALT patients and 75% for TERT-L/non-ALT patients, while 10-year OS was 22% for TERT-H, 24% for ALT, and 75% for TERT-L/non-ALT (Table. 2). All patients with TERT-L/non-ALT tumors who died had RIN values > 6.5, ruling out low RNA integrity as a cause for low TERT expression by RNA sequencing. Consistent with previous studies, the presence of *ALK* and *RAS/TP53* pathway alterations (Supplementary Fig. S12A and S12B) (27,38) and diploid DNA content (Supplementary Fig. S12C and S12D) were associated with poor outcome in these high-risk patients.

Unlike OS, EFS was not substantially different among the three groups defined by *TERT* expression and ALT status ($P = 0.137$; Fig. 2D). Therefore, we assessed OS in only those patients who experienced an event, and observed that while TERT-H and ALT patients had abysmal OS following an event, patients in the TERT-L/non-ALT group had significantly higher OS than patients in the TERT-H or ALT groups (log-rank test comparing three groups: $P < 0.001$; Fig. 2E). These data suggest that the differences in OS likely represent differences in the success of salvage therapy following an event.

Consistent with previous findings for high-risk patients, there was no difference in EFS ($P = 0.68$; Supplementary Fig. S13A) or OS ($P = 0.46$; Supplementary Fig. S13B) between *MYCN*-Amp and non-*MYCN*-Amp patients (39,40). Even though the majority of *MYCN*-

Amp tumors had high *TERT* expression and belonged to the TERT-H group (n=22), some *MYCN*-Amp tumors had low *TERT* expression (n=7; Supplementary Fig. S9A) and were classified as TERT-L. Notably, *MYCN*-Amp patients in the TERT-H group had a lower 5-year OS (29%) relative to the 86% seen for patients with *MYCN*-Amp & TERT-L tumors (P = 0.013; Fig. 2F). This observation was further validated in the SEQC dataset (https://hgserver1.amc.nl/cgi-bin/r2/main.cgi); *MYCN*-Amp tumors with low *TERT* expression had a significantly higher OS compared to *MYCN*-Amp tumors with high *TERT* expression (P = 0.0053; Supplementary Fig. S13C). Multivariate cox-regression analysis demonstrated that high *TERT* expression or ALT positivity predict poor OS but not EFS, independent of *MYCN* amplification, ploidy, *ALK* status, *RAS/TP53* pathway alterations, or chromosome arm 11q deletion (Fig. 3A and 3B).

As median cutoff may not be optimal for distinguishing *TERT* expressing and non-expressing tumors for biological classification, we also defined a *TERT* expression threshold that separates *TERT* positive and *TERT* negative tumors by fitting a bimodal normal distribution (Fig. S14 A and B), as described previously (27). Based on the latter *TERT* expression threshold, 16/107 (14.9%) high-risk tumors were classified as *TERT* expression low and negative for the C-circle ALT marker (TERT&ALT-). Overall survival but not Event-free survival was significantly different for ALT, TERT positive and TERT&ALT-tumors (log-rank test comparing three groups: P = 0.022; Fig. S14C and S14D), results comparable to using median *TERT* expression for the cutoff (Fig. 2C).

Taken together, we classified high-risk neuroblastoma patients into 3 subgroups based on *TERT* expression and ALT status. Non-ALT patients with lower *TERT* expression were associated with superior overall survival when compared to patients with ALT phenotype or higher *TERT* expression, irrespective of other known risk factors.

High Telomere Content is Not Limited to the ALT phenotype in High-Risk Neuroblastoma

To investigate whether ALT is associated with high telomere content (TC) as described previously (14,15,26,41), we assessed relative TC using telomeric qPCR in 134 neuroblastoma samples for which both ALT status and *TERT* expression were known. As expected, ALT tumors had higher relative TC than TERT-H (Wilcoxon $P = 1.87\times10^{-11}$), TERT-L/non-ALT (Wilcoxon $P = 9.5\times10^{-4}$), or non-high-risk tumors (Wilcoxon $P = 5.54\times10^{-8}$; Fig. 4A). Consistent with primary patient tumors, ALT cell lines and PDXs had higher relative TC than non-ALT models (Supplementary Fig. S15A-C and Table S2; Wilcoxon $P = 2.55\times10^{-5}$). ALT neuroblastoma cell lines were also associated with high and heterogeneous telomere length relative to telomerase-positive cell lines, as detected by telomere restriction fragment (TRF) length analysis (mean TRF length >20kb; Supplementary Fig. S15C) and by telomere fluorescence *in-situ* hybridization on metaphase spreads (Supplementary Fig. S15D).

TERT-L/non-ALT tumors and non-high-risk tumors were each significantly associated with a much higher relative TC when compared to TERT-H tumors (Wilcoxon $P = 2.6\times10^{-07}$; Supplementary Fig. 4A). As WGS data was available for 85/134 samples, we measured telomere DNA abundance (TTAGGG/CCCTAA canonical repeats) from short-read WGS for each tumor and from a blood sample from each patient, and demonstrated a significant

correlation between tumor telomere content measured by qPCR and WGS (Supplementary Fig. S16A; Spearman Rho = 0.701; $P = 5.87\times10^{-14}$). We observed that 11/17 TERT-L/non-ALT tumors had increased telomere content (tumor/blood ratio > 1; Supplementary Fig. S16B) and of 82 non-ALT high-risk tumor samples with age > 18 months, 16 tumors had high TC, similar in range to that observed within ALT tumors (relative TC >5; corresponds to mean TRF length > 20 kb; Supplementary Table S1). This non-ALT high TC group meets the phenotypic criteria of the previously defined EST phenotype (26).

In the 16 tumors with high TC, 12 had low *TERT* expression and 4 had high *TERT* expression (Supplementary Table S1). To validate that TERT-L&C-circle- tumors with high telomere content (TC>5) are ALT-negative, we assessed APBs in 34 primary patient tumors (12 tumors in the TERT-L&C-circle- group with TC>5, 11 tumors in TERT-L&C-circle- group with TC<5, and 10 C-circle+ tumors). APBs were detected in 3/12 TERT-L&C-circle- tumors with TC>5, while 0/11 tumors in TERT-L&C-circle- group with TC<5 were APB-positive. In C-circle positive tumors, 8/10 were positive for APBs (Supplementary Table S1, Supplementary Fig. S17). Thus, the C-circle assay missed detection of ALT in 3/11 low TERT tumors with high TC, while the APB assay did not detect ALT in 2/10 C-circle positive tumors.

We compared clinical outcome between the 28/107 ALT tumors with ALT defined as either C-circle+ or APB+) and the 9/79 non-ALT tumors that had low *TERT* expression and TC>5 (Fig. 4B). OS among these two groups was significantly different, with the ALT cohort having a much worse outcome ($P = 0.007$; Fig. 4C).

We also measured relative TC content, C-circles, and *TERT* mRNA in 104 neuroblastoma cell lines and 28 PDXs (Supplementary Table S2). We identified 5 neuroblastoma cell lines (LA-N-6, COG-N-291, CHLA-132, COG-N-509hnb, and COG-N-562hnb) and 2 PDXs (COG-N-518x and COG-N-649x) with low *TERT* expression that were ALT negative (Fig. 4D) and had relative TC>5 (Supplementary Table S2), i.e. consistent with the EST phenotype (26). We validated the lack of ALT activation in these models by confirming a low frequency of APBs (Supplementary Fig. S18A and S18B). All the EST cell lines and PDXs lacked telomerase activity by TRAP assay (Fig. 4E) and had high telomere length using TRF analysis in cell lines (mean TRF length > 20 kb; Fig. 4F), and telomere/centromere FISH in PDXs (Fig. 4G) and showed high and heterogeneous telomere lengths (Fig. 4G; Supplementary Fig. S18C) with a lower frequency of telomere-signal-free chromosomal ends than ALT cell lines (Wilcoxon $P = 3.35\times10^{-07}$; Supplementary Fig. S18C and S18D). Unlike ALT tumors, where *ATRX/DAXX* genomic alterations are common (14,15), none of the TERT-L/non-ALT tumor samples with TC>5 (n=14) had genomic alterations in *ATRX, DAXX, H3F3A* or *SMARCAL1*. Consistent with the patient samples, the TERT-L/non-ALT cell lines and PDXs with TC>5 expressed full-length wild-type ATRX and DAXX protein (Supplementary Fig. S19A and S19B).

We were able to induce the ALT-specific marker C-circles in the EST cell line LA-N-6 (but not in the telomerase-positive cell line SK-N-BE (2)) by stable ATRX knockdown using shRNA (Supplementary Fig. S20A and S20B). Knockdown of ATRX in LA-N-6 also

increased APBs in these cells (Supplementary Fig. S20C and S20D). This suggests that ALT repressors such as ATRX can block activation of ALT in TERT-L/non-ALT tumors.

Thus, some neuroblastomas stratified clinically as high-risk have high TC despite no apparent activation of classical ALT markers or TERT expression, and as shown in Figure 3C, this phenotypic subset has a much more favorable OS probability than the ALT tumors.

Continuous Shortening of Telomeres in TERT-L/Non-ALT Cell Lines Established from High-Risk Neuroblastoma Patients

Roughly 15% of the high-risk neuroblastoma tumor samples were negative for *TERT* expression without any evidence of ALT activation (TERT- & ALT -; Supplementary Fig. S14 A). To investigate whether this phenotype was associated with yet another uncharacterized telomere maintenance mechanism, we measured the change in telomere length across multiple passages in 3 neuroblastoma TERT- & ALT- cell lines established from high-risk patients (LA-N-6, COG-N-346h, and COG-N-387h). All three cell lines had very low *TERT* expression, were negative for telomerase activity, and lacked ALT-specific markers (Supplementary Table S2); LA-N-6 is a non-*MYCN*-Amp neuroblastoma cell line with TC>5, COG-N-346h is a non-*MYCN*-Amp neuroblastoma cell line with TC<5, and COG-N-387h is a *MYCN*-Amp neuroblastoma cell line with TC<5 (Supplementary Table S2). All three cell lines showed continuous shortening of telomere length by TRF analysis across progressive passages (Fig. 5A); shortening of telomeres was verified as a reduction in telomere content by qPCR (Fig. 5B). All three TERT- & ALT- lines remained C-circle-negative (Supplementary Fig. S21A) and TERT-low across those same passages in culture (Supplementary Fig. S21B).

We observed a substantial decline in cell viability in 2 of 3 EST cell lines following several passages *in vitro* (Fig. 5C). Interestingly, the decline in viability of LA-N-6, a cell line with very high telomere content, was minimal even after 40 passages (Fig. 5C).

Taken together our data suggest that patients with TERT-L/non-ALT tumors derive a survival advantage from the failure of their tumors to maintain telomere length, but that some of these tumors may develop as yet unknown mechanisms to overcome this limitation.

Discussion

We report here a comprehensive analysis of telomere maintenance mechanisms (TMM) in high-risk neuroblastoma in the context of tumor genomics and clinical outcome. Consistent with previous studies, we confirmed using the ALT-specific C-circle assay that ALT is activated in 23% of high-risk neuroblastoma tumors (26). ALT patient tumors, cell lines, and PDXs expressed very low *TERT* mRNA, indicating ALT and telomerase activation occur in a mutually exclusive manner.

ATRX genomic alterations have been associated with the ALT phenotype in neuroblastoma (15,27), but the relationship of ALT (using a specific marker) to *ATRX* genomic alterations has not been precisely defined. We observed *ATRX* structural variants, in frame fusions and single nucleotide variants in 60% of ALT tumors, but the remainder lacked any identifiable

genomic lesions previously reported to be associated with the ALT phenotype. Consistent with previous reports that *ATRX* mutations are often enriched in older patients (15), the ALT patients in our cohort had a late disease onset irrespective of *ATRX* status. Patients with ALT phenotype had a poor overall survival, irrespective of *ATRX* status.

High telomere content has been associated with ALT (15,37,41), but we confirmed a previous report that long telomeres are not exclusive to ALT tumors in high-risk neuroblastoma (26), as 16% of the ALT-negative high-risk tumors had total telomere content as high as that seen in the ALT-positive tumors. Thus, assessment of ALT status using high telomere content as measured by FISH, WGS/WES, or qPCR would over-estimate the frequency of ALT in neuroblastoma.

Similar to previous reports, we identified *TERT* structural variants (*TERT*$^{SV+}$) in ~20% of high-risk neuroblastoma patients, and all *TERT*$^{SV+}$ tumors had highly upregulated *TERT* mRNA (5,11). Among tumors with *MYCN* genomic amplification (*MYCN*-Amp), a sub-population had *TERT* expression as low as that seen in ALT tumors. Using neuroblastoma cell lines, we showed that MYCN overexpression enhanced *TERT* mRNA expression in a *TERT*-expressing non-*MYCN*-Amp neuroblastoma cell line without *TERT*$^{SV+}$, but failed to induce TERT activation in cell lines with *TERT*$^{SV+}$ or in *TERT* non-expressing cell lines. Thus, MYCN overexpression by itself might not be always sufficient to transcriptionally activate *TERT*.

As seen in a recent study (27), we observed that *TERT* activation in high-risk neuroblastoma was not limited to tumors with *TERT*$^{SV+}$ and *MYCN* amplification, as some tumors without these alterations expressed *TERT* as highly as *TERT*$^{SV+}$ and *MYCN*-Amp tumors. The prior study quantified *TERT* mRNA expression by microarray and detected ALT activation by scoring APBs on tumor tissue sections (27,42), and reported that only 3 of 90 high-risk tumors lacked a TMM (42). By employing RNA sequencing (validated by qRT-PCR) for *TERT* expression and the C-circle assay to detect ALT, we found that 12 to 26% (depending on the cutoff employed) of high-risk neuroblastoma tumors (including some *MYCN*-Amp tumors) had low TERT expression and lacked ALT activation, and those patients had a significantly better overall survival. Consistent with this latter observation high-risk neuroblastoma cell lines that were non-ALT, low *TERT* expressing, and lacked telomerase activity showed continuous shortening of telomeres with growth *in vitro* and 2 of 3 TERT-L/non-ALT cell lines spontaneously lost viability after multiple passages in culture.

By combining analysis of ALT status (by C-circles) and *TERT* mRNA expression as measured by RNA-seq we were able to classify high-risk neuroblastoma patients into 3 subgroups based on TMM (TERT-H, ALT, and TERT-L/non-ALT). The 10-year overall survival (OS) in high-risk patients with TERT-H and ALT tumors was < 25% while the TERT-L/non-ALT group had a 75% 10-year OS, despite being classified as high-risk based on current risk stratification protocols (43). We also showed that OS for patients with *MYCN* amplification was significantly higher if the tumors had low *TERT* expression, which might explain the extreme dichotomy in the clinical course of *MYCN*-Amp patients (44).

We observed that *TERT* high-expressing and ALT neuroblastomas have poor clinical outcomes comprising uniform cohorts of true high-risk patients. An important and novel observation was our demonstration that 12 to 26% of clinically high-risk neuroblastomas lacked a TMM and while those had EFS comparable to *TERT*-high and ALT patients, TMM-negative patients had a significantly higher long-term overall survival (75%). Based on our data, we hypothesize that TMM-negative tumors develop chemo-resistance and progress similarly to TMM-positive tumors, but due to a lack of TMM they continue to erode telomeres which eventually enables salvage therapy given after disease progression to eradicate the tumors. Thus, current standard of care for high-risk neuroblastoma patients that relies on dose-intensive cytotoxic chemotherapy in as short a time frame as possible may not be optimal for TMM-negative high-risk patients, and alternative strategies such as longer time frame low dose chemotherapy should be tested in future clinical trials.

Employing the C-circle assay, considered to be specific for ALT cells and known to be a quantitative marker for ALT activity (13,45), enabled us to identify ALT in 23% of high-risk (age >18 months) neuroblastoma patients, and these patients had a low overall survival (Fig. 2). However, 3 tumors with high telomere content were positive for APBs but had a C-circle content below cutoff, which suggested that some ALT tumors may be missed by implementing only the C-circle assay as marker for detection of ALT. We analyzed clinical outcome for patients with low TERT expression and high telomere content with ALT defined as C-circle positive or APB positive and we observed an apparent higher overall survival for TMM-negative patients identified by employing both assays to define ALT-positivity (comparing Fig. 2c to Fig. 4c). APB analysis alone did not detect all ALT tumors as we identified 2 *ATRX* mutant C-circle positive tumors that were APB negative, indicating that APBs have limitations in detecting ALT tumors, which is consistant with a previous report (14). Additionally, APBs have the limitation of also being detectable in non-ALT cells (45). Cell lines with long telomeres resulting from forced telomerase overexpression have APBs (28), suggesting that APBs are associated with long telomeres rather than being specific for the ALT mechanism (45). Future studies in a large cohort of patients will be necessary to determine the optimal approach for TMM classification of tumors that have low TERT expression and a high telomere content.

Using the C-circle assay, we observed that patients with ALT positive tumors had a dismal overall survival, with no difference in overall survival between ALT and TERT positive patients, which is consistent with previous reports that *ATRX* altered high risk tumors (all of which were ALT) were associated with very poor overall survival (15,33). Roderwieser and colleagues reported a substantially better overall survival for ALT neuroblastoma compared to TERT activated patients (42). We suggest that the difference in clinical outcome between our study and the prior study could be due to our use of the C-circle assay compared to use of APB's to identify ALT, differences in risk and age groups (our study focused on HR samples in patients with age > 18 months), and length of clinical follow-up, as ALT tumors tend to have an indolent phenotype (15,46). Additionally, our study here reported higher frequency of ALT & TERT negative tumors, which may be due to use of different methods to assess TERT, different TERT expression cutoffs, inclusion of only high risk patients with age > 18 months, and differences in classification of low-*TERT* expressing *MYCN* amplified tumors.

A strength of our study is the relatively large sample size of stage 4 high-risk neuroblastoma patients diagnosed at age > 18 months, representing patients receiving intense chemotherapy at high risk for a poor clinical outcome (43). Another strength of our study is that we determined *TERT* mRNA expression in the patient samples using RNA-sequencing, which may be more robust than microarray technology for quantifying low-abundance transcripts such as that of *TERT*, as suggested previously (47). A limitation of our study is that TERT expression is a continuous variable and cutoffs for high vs low expression using different approaches give comparable results. Our results need to be validated in a large cohort of patients, which will also allow optimizing the cutoff for TERT expression. While *TERT* mRNA expression could be affected by RNA integrity or tumor cell content, both of which were controlled for in this study, which is important to prevent classifying a tumor as TERT low inappropriately. Another limitation of our study and of previous studies that assessed telomere maintenance is that the patients studied were not from a uniformly treated group of patients receiving the most current standard-of-care therapies. Thus, it will be important to confirm our observations in a validation cohort of high-risk neuroblastoma patients receiving uniform therapy on current protocols.

In summary, we demonstrated that quantifying *TERT* mRNA and C-circle abundance enables classifying high-risk neuroblastoma patients into 3 subgroups that have distinct clinical outcomes, independent of currently employed risk-stratification methods, including *MYCN* amplification. TMM-positive (TERT high-expressing and ALT) neuroblastomas are true high-risk tumors, each with distinct, potentially targetable molecular pathways required for maintaining telomeres. Therapeutic strategies targeting telomerase and ALT activation warrant investigation in TMM-positive neuroblastomas (30,48,49). An important and novel observation is our demonstration that clinically high-risk patients with TMM-negative tumors have an exceptionally high overall survival, which is likely due to the eventual success of therapy (combined with telomere erosion) even after disease progression. If future studies confirm the latter observation, stratification of patients based on TMM using robust markers (TERT mRNA expression and DNA C-circles) will improve the analysis of future clinical trials, and a reduction in the intensity of therapy may be attainable for TMM-negative patients.

Supplementary Material

Refer to Web version on PubMed Central for supplementary material.

Acknowledgments

We thank the NCI Pediatric Preclinical Testing Consortium for providing some of the PDX sequencing data, the Children's Oncology Group (COG) Neuroblastoma Biobank for tumor samples and clinical data, and the COG Childhood Cancer Repository (www.CCCells.org), supported by Alex's Lemonade Stand, for providing cell lines and PDXs for this study. We thank the patients and their families for donating samples to enable this research.

Financial Support: Cancer Prevention & Research Institute of Texas RP170510 (to CPR), National Cancer Institute (NCI) CA217251 (to CPR), NCI CA221957 (to CPR), NCI R01CA204974 (to SJD), NCI R35CA220500 (to JMM), the US National Institutes of Health grants RC1MD004418 to the TARGET consortium, CA98543 and CA98413 to the Children's Oncology Group, Alex's Lemonade Stand Foundation for support of the COG Childhood Cancer Repository (www.CCcells.org) and the Roberts Collaborative for Genetics and Individualized Medicine (to GL).

References

1. Hanahan D, Weinberg RA. Hallmarks of cancer: the next generation. Cell 2011;144:646–74. [PubMed: 21376230]
2. Kim NW, Piatyszek MA, Prowse KR, Harley CB, West MD, Ho PL, et al. Specific association of human telomerase activity with immortal cells and cancer. Science (New York, NY) 1994;266:2011–5.
3. Cong YS, Wright WE, Shay JW. Human telomerase and its regulation. Microbiol Mol Biol Rev 2002;66:407–25, table of contents. [PubMed: 12208997]
4. Takakura M, Kyo S, Kanaya T, Hirano H, Takeda J, Yutsudo M, et al. Cloning of human telomerase catalytic subunit (hTERT) gene promoter and identification of proximal core promoter sequences essential for transcriptional activation in immortalized and cancer cells. Cancer research 1999;59:551–7. [PubMed: 9973199]
5. Peifer M, Hertwig F, Roels F, Dreidax D, Gartlgruber M, Menon R, et al. Telomerase activation by genomic rearrangements in high-risk neuroblastoma. Nature 2015;526:700–4. [PubMed: 26466568]
6. Huang FW, Hodis E, Xu MJ, Kryukov GV, Chin L, Garraway LA. Highly recurrent TERT promoter mutations in human melanoma. Science 2013;339:957–9. [PubMed: 23348506]
7. Landa I, Ganly I, Chan TA, Mitsutake N, Matsuse M, Ibrahimpasic T, et al. Frequent somatic TERT promoter mutations in thyroid cancer: higher prevalence in advanced forms of the disease. J Clin Endocrinol Metab 2013;98:E1562–6. [PubMed: 23833040]
8. Killela PJ, Reitman ZJ, Jiao Y, Bettegowda C, Agrawal N, Diaz LA Jr., et al. TERT promoter mutations occur frequently in gliomas and a subset of tumors derived from cells with low rates of self-renewal. Proc Natl Acad Sci U S A 2013;110:6021–6. [PubMed: 23530248]
9. Borah S, Xi L, Zaug AJ, Powell NM, Dancik GM, Cohen SB, et al. Cancer. TERT promoter mutations and telomerase reactivation in urothelial cancer. Science 2015;347:1006–10. [PubMed: 25722414]
10. Wang N, Xu D, Sofiadis A, Hoog A, Vukojevic V, Backdahl M, et al. Telomerase-dependent and independent telomere maintenance and its clinical implications in medullary thyroid carcinoma. J Clin Endocrinol Metab 2014;99:E1571–9. [PubMed: 24758186]
11. Valentijn LJ, Koster J, Zwijnenburg DA, Hasselt NE, van Sluis P, Volckmann R, et al. TERT rearrangements are frequent in neuroblastoma and identify aggressive tumors. Nat Genet 2015;47:1411–4. [PubMed: 26523776]
12. Heaphy CM, Subhawong AP, Hong SM, Goggins MG, Montgomery EA, Gabrielson E, et al. Prevalence of the alternative lengthening of telomeres telomere maintenance mechanism in human cancer subtypes. Am J Pathol 2011;179:1608–15. [PubMed: 21888887]
13. Henson JD, Cao Y, Huschtscha LI, Chang AC, Au AY, Pickett HA, et al. DNA C-circles are specific and quantifiable markers of alternative-lengthening-of-telomeres activity. Nat Biotechnol 2009;27:1181–5. [PubMed: 19935656]
14. Heaphy CM, de Wilde RF, Jiao Y, Klein AP, Edil BH, Shi C, et al. Altered telomeres in tumors with ATRX and DAXX mutations. Science (New York, NY) 2011;333:425.
15. Cheung NK, Zhang J, Lu C, Parker M, Bahrami A, Tickoo SK, et al. Association of age at diagnosis and genetic mutations in patients with neuroblastoma. JAMA 2012;307:1062–71. [PubMed: 22416102]
16. Lovejoy CA, Li W, Reisenweber S, Thongthip S, Bruno J, de Lange T, et al. Loss of ATRX, genome instability, and an altered DNA damage response are hallmarks of the alternative lengthening of telomeres pathway. PLoS Genet 2012;8:e1002772. [PubMed: 22829774]
17. Sturm D, Witt H, Hovestadt V, Khuong-Quang DA, Jones DT, Konermann C, et al. Hotspot mutations in H3F3A and IDH1 define distinct epigenetic and biological subgroups of glioblastoma. Cancer Cell 2012;22:425–37. [PubMed: 23079654]
18. Diplas BH, He X, Brosnan-Cashman JA, Liu H, Chen LH, Wang Z, et al. The genomic landscape of TERT promoter wildtype-IDH wildtype glioblastoma. Nat Commun 2018;9:2087. [PubMed: 29802247]
19. Maris JM, Hogarty MD, Bagatell R, Cohn SL. Neuroblastoma. Lancet 2007;369:2106–20. [PubMed: 17586306]

20. Maris JM. Recent advances in neuroblastoma. The New England journal of medicine 2010;362:2202–11. [PubMed: 20558371]
21. Park JR, Kreissman SG, London WB, Naranjo A, Cohn SL, Hogarty MD. A phase III randomized clinical trial (RCT) of tandem myeloablative autologous stem cell transplant (ASCT) using peripheral blood stem cell (PBSC) as consolidation therapy for high-risk neuroblastoma (HR-NB): A Children's Oncology Group (COG) study. Journal of Clinical Oncology 2016;34.
22. Park JR, Kreissman SG, London WB, Naranjo A, Cohn SL, Hogarty MD, et al. Effect of Tandem Autologous Stem Cell Transplant vs Single Transplant on Event-Free Survival in Patients With High-Risk Neuroblastoma: A Randomized Clinical Trial. JAMA 2019;322:746–55. [PubMed: 31454045]
23. Mosse YP, Laudenslager M, Longo L, Cole KA, Wood A, Attiyeh EF, et al. Identification of ALK as a major familial neuroblastoma predisposition gene. Nature 2008;455:930–5. [PubMed: 18724359]
24. Pugh TJ, Morozova O, Attiyeh EF, Asgharzadeh S, Wei JS, Auclair D, et al. The genetic landscape of high-risk neuroblastoma. Nature genetics 2013;45:279–84. [PubMed: 23334666]
25. Hertwig F, Peifer M, Fischer M. Telomere maintenance is pivotal for high-risk neuroblastoma. Cell Cycle 2016;15:311–2. [PubMed: 26653081]
26. Dagg RA, Pickett HA, Neumann AA, Napier CE, Henson JD, Teber ET, et al. Extensive Proliferation of Human Cancer Cells with Ever-Shorter Telomeres. Cell Rep 2017;19:2544–56. [PubMed: 28636942]
27. Ackermann S, Cartolano M, Hero B, Welte A, Kahlert Y, Roderwieser A, et al. A mechanistic classification of clinical phenotypes in neuroblastoma. Science 2018;362:1165–70. [PubMed: 30523111]
28. Pickett HA, Cesare AJ, Johnston RL, Neumann AA, Reddel RR. Control of telomere length by a trimming mechanism that involves generation of t-circles. The EMBO journal 2009;28:799–809. [PubMed: 19214183]
29. Lopez G, Conkrite KL, Doepner M, Rathi KS, Modi A, Vaksman Z, et al. Structural variation targets neurodevelopmental genes and identifies SHANK2 as a tumor suppressor in neuroblastoma. bioRxiv 2019.
30. Flynn RL, Cox KE, Jeitany M, Wakimoto H, Bryll AR, Ganem NJ, et al. Alternative lengthening of telomeres renders cancer cells hypersensitive to ATR inhibitors. Science 2015;347:273–7. [PubMed: 25593184]
31. Viceconte N, Dheur MS, Majerova E, Pierreux CE, Baurain JF, van Baren N, et al. Highly Aggressive Metastatic Melanoma Cells Unable to Maintain Telomere Length. Cell Rep 2017;19:2529–43. [PubMed: 28636941]
32. Mender I, Shay JW. Telomere Restriction Fragment (TRF) Analysis. Bio Protoc 2015;5.
33. Molenaar JJ, Koster J, Zwijnenburg DA, van Sluis P, Valentijn LJ, van der Ploeg I, et al. Sequencing of neuroblastoma identifies chromothripsis and defects in neuritogenesis genes. Nature 2012;483:589–93. [PubMed: 22367537]
34. Yeager TR, Neumann AA, Englezou A, Huschtscha LI, Noble JR, Reddel RR. Telomerase-negative immortalized human cells contain a novel type of promyelocytic leukemia (PML) body. Cancer research 1999;59:4175–9. [PubMed: 10485449]
35. Farooqi AS, Dagg RA, Choi LM, Shay JW, Reynolds CP, Lau LM. Alternative lengthening of telomeres in neuroblastoma cell lines is associated with a lack of MYCN genomic amplification and with p53 pathway aberrations. J Neurooncol 2014;119:17–26. [PubMed: 24792489]
36. Rokita JL, Rathi KS, Cardenas MF, Upton KA, Jayaseelan J, Cross KL, et al. Genomic Profiling of Childhood Tumor Patient-Derived Xenograft Models to Enable Rational Clinical Trial Design. Cell Rep 2019;29:1675–89 e9. [PubMed: 31693904]
37. Lundberg G, Sehic D, Lansberg JK, Ora I, Frigyesi A, Castel V, et al. Alternative lengthening of telomeres--an enhanced chromosomal instability in aggressive non-MYCN amplified and telomere elongated neuroblastomas. Genes Chromosomes Cancer 2011;50:250–62. [PubMed: 21319260]
38. Bresler SC, Weiser DA, Huwe PJ, Park JH, Krytska K, Ryles H, et al. ALK mutations confer differential oncogenic activation and sensitivity to ALK inhibition therapy in neuroblastoma. Cancer Cell 2014;26:682–94. [PubMed: 25517749]

39. Rajbhandari P, Lopez G, Capdevila C, Salvatori B, Yu J, Rodriguez-Barrueco R, et al. Cross-Cohort Analysis Identifies a TEAD4-MYCN Positive Feedback Loop as the Core Regulatory Element of High-Risk Neuroblastoma. Cancer Discov 2018;8:582–99. [PubMed: 29510988]
40. Campbell K, Gastier-Foster JM, Mann M, Naranjo AH, Van Ryn C, Bagatell R, et al. Association of MYCN copy number with clinical features, tumor biology, and outcomes in neuroblastoma: A report from the Children's Oncology Group. Cancer 2017;123:4224–35. [PubMed: 28696504]
41. Onitake Y, Hiyama E, Kamei N, Yamaoka H, Sueda T, Hiyama K. Telomere biology in neuroblastoma: telomere binding proteins and alternative strengthening of telomeres. J Pediatr Surg 2009;44:2258–66. [PubMed: 20006006]
42. Roderwieser A, Sand F, Walter E, Fischer J, Gecht J, Bartenhagen C, et al. Telomerase Is a Prognostic Marker of Poor Outcome and a Therapeutic Target in Neuroblastoma. JCO Precision Oncology 2019:1–20.
43. Cohn SL, Pearson AD, London WB, Monclair T, Ambros PF, Brodeur GM, et al. The International Neuroblastoma Risk Group (INRG) classification system: an INRG Task Force report. J Clin Oncol 2009;27:289–97. [PubMed: 19047291]
44. Kushner BH, Modak S, Kramer K, LaQuaglia MP, Yataghene K, Basu EM, et al. Striking dichotomy in outcome of MYCN-amplified neuroblastoma in the contemporary era. Cancer 2014;120:2050–9. [PubMed: 24691684]
45. Henson JD, Reddel RR. Assaying and investigating Alternative Lengthening of Telomeres activity in human cells and cancers. FEBS Lett 2010;584:3800–11. [PubMed: 20542034]
46. Kurihara S, Hiyama E, Onitake Y, Yamaoka E, Hiyama K. Clinical features of ATRX or DAXX mutated neuroblastoma. J Pediatr Surg 2014;49:1835–8. [PubMed: 25487495]
47. Ceccarelli M, Barthel FP, Malta TM, Sabedot TS, Salama SR, Murray BA, et al. Molecular Profiling Reveals Biologically Discrete Subsets and Pathways of Progression in Diffuse Glioma. Cell 2016;164:550–63. [PubMed: 26824661]
48. Zheng XH, Nie X, Fang Y, Zhang Z, Xiao Y, Mao Z, et al. A Cisplatin Derivative Tetra-Pt(bpy) as an Oncotherapeutic Agent for Targeting ALT Cancer. J Natl Cancer Inst 2017;109.
49. Mender I, Gryaznov S, Dikmen ZG, Wright WE, Shay JW. Induction of telomere dysfunction mediated by the telomerase substrate precursor 6-thio-2'-deoxyguanosine. Cancer Discov 2015;5:82–95. [PubMed: 25516420]

Significance

Findings assess telomere maintenance mechanisms with TERT mRNA and the ALT DNA biomarker C-circles to stratify neuroblastoma into 3 groups with distinct overall survival independent of currently used clinical risk classifiers.

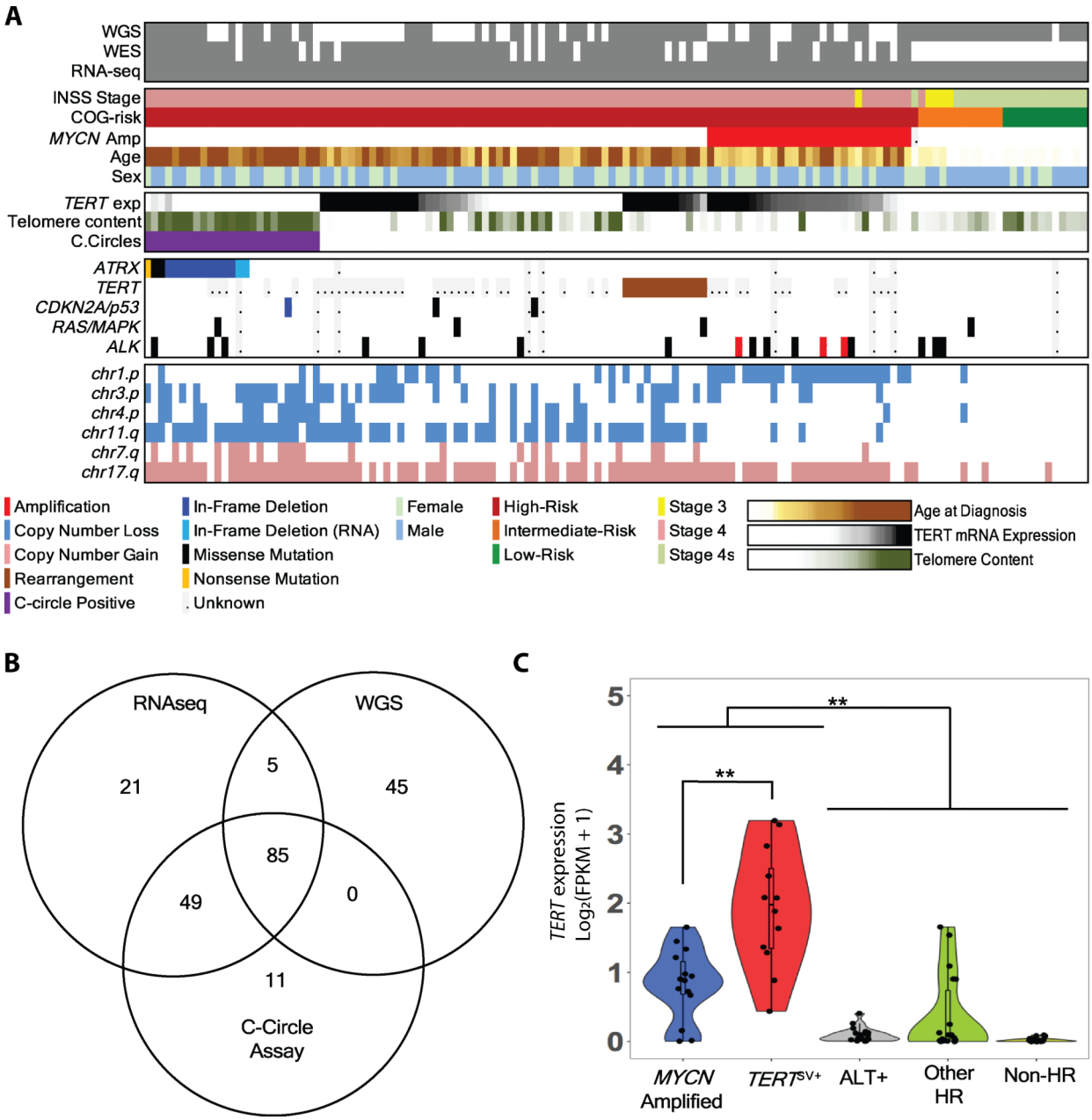

Figure. 1. Alternative lengthening of telomeres (ALT) and TERT activation in neuroblastoma.

(A) Data tracks genome sequencing and RNA-seq availability, clinical variables, presence of C-circles, telomere content, *TERT* mRNA expression by RNA-seq, *ATRX* genomic alterations, TERT rearrangements, CDKN2A/p53 pathway alterations, Ras/MAPK alterations, *ALK* genomic alterations and the most common copy number alterations in n = 134 primary neuroblastoma pre-treated samples. (B) RNA-seq, WGS, and C-circle assay data overlap in neuroblastoma primary patient tumors. (C) *TERT* expression in primary neuroblastoma samples with WGS, RNA-seq, and C-circle assay (n=85). Tumors were subcategorized based on presence of *MYCN* amplification (blue; n = 15), *TERT* structural variants (red; n = 12), ALT activation (grey; n = 18), other high-risk neuroblastoma without

these alterations (green; $n = 17$), and non-high-risk neuroblastoma (yellow; $n = 23$). **: $P<0.01$; P-value was determined using Wilcoxon rank-sum test.

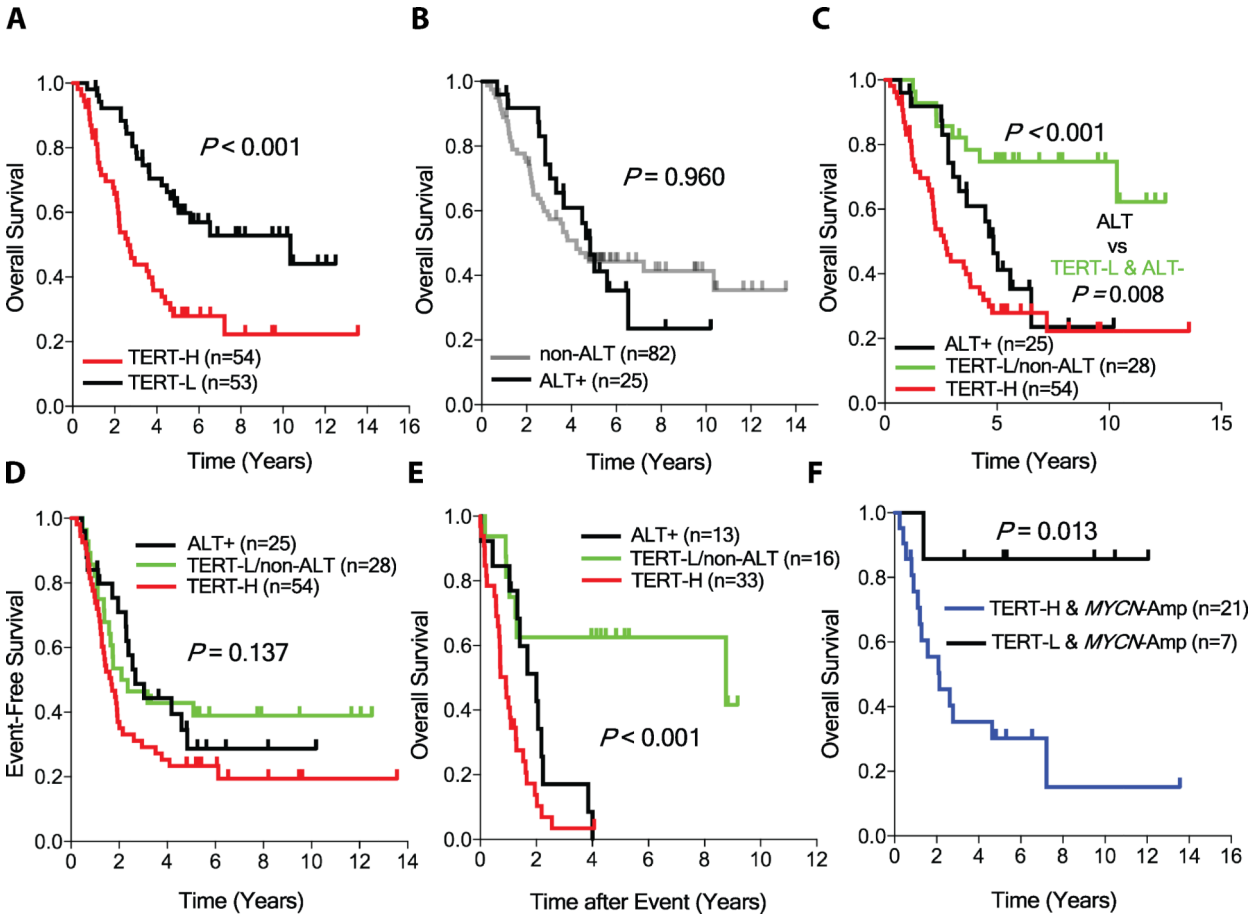

Figure. 2. *TERT* expression in combination with ALT status predicts overall survival in high-risk neuroblastoma.

(A) Kaplan-Meier overall survival curves of high-risk neuroblastoma patients (n=107) based on *TERT* expression. The patients were divided into *TERT*-high (TERT-H, n = 54; red) and *TERT*-low (TERT-L, n = 53; black) according to the median *TERT* mRNA expression level assessed by RNA sequencing. (B) Kaplan-Meier overall survival curves of high-risk NB patients based on presence (black) or absence (grey) of C-circles, an ALT-specific biomarker. (C) Kaplan-Meier overall survival curves of the same samples presented in Figs 2A and 2B, combining *TERT* expression with ALT status. As all the ALT patients (black) were a subgroup of TERT-L group, splitting the TERT-L group by ALT status subcategorizes high-risk neuroblastoma patients into three groups (TERT-H, ALT and TERT-L/non-ALT). (D) Kaplan-Meier event-free survival curves of the same patients presented in Fig 2C. (E) Kaplan-Myer overall survival curves for patients from 2C who had an event. (F) Kaplan-Meier overall survival curves in *MYCN*-Amp patients based on *TERT* expression. *TERT*-H & *MYCN*-Amp patients shown in blue, and *TERT*-L & *MYCN*-Amp patients shown in black. *P*-value was determined using the log-rank test.

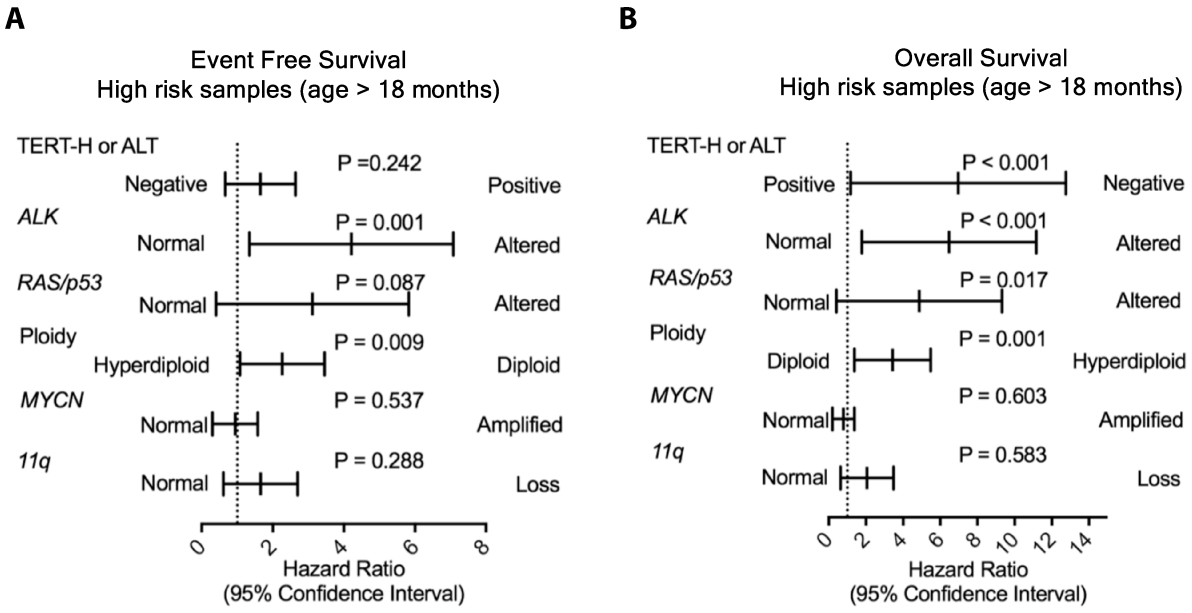

Figure. 3. High TERT expression or ALT activation are associated with poor overall survival irrespective of other risk factors.

Multivariate Cox regression analysis for (A) event-free survival and (B) overall survival based on high *TERT* mRNA expression or ALT activation, *ALK* genomic alterations, *RAS/TP53*-pathway genomic alterations, ploidy, *MYCN* amplification and 11q chromosomal loss.

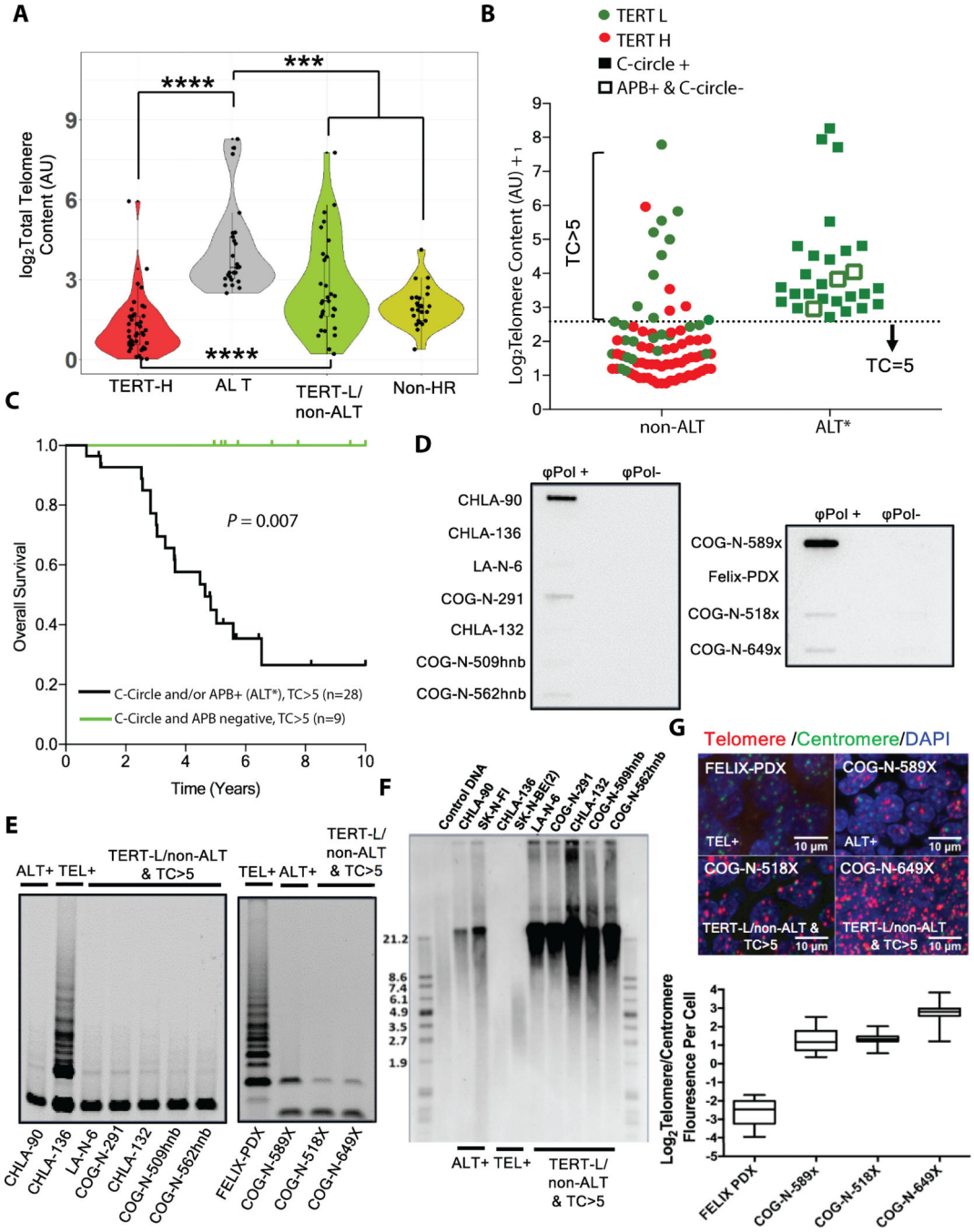

Figure. 4. High telomere content in non-ALT, TERT low-expressing high-risk neuroblastoma primary patient tumor samples, neuroblastoma cell lines, and patient-derived xenografts.

(A) Relative total telomere content (TC), in arbitrary units (AU), measured by qPCR in primary patient tumors in TERT-H ($n = 55$), ALT ($n = 25$), TERT-L/non-ALT ($n = 30$), and non-high-risk tumors ($n = 25$). (B) Relative telomere content in ALT* versus non-ALT high-risk neuroblastoma tumors. The horizontal line demarcates TC=5, which corresponds to telomere length >20kb. (C) Overall survival of patients in the TERT-L group with high telomere content (TC>5), separated based on ALT* status with ALT defined as positive for C-circles or APBs (D). Confirmatory C-circle assay for LA-N-6, COG-N-291, CHLA-132,

COG-N-509hnb and COG-N-562hnb Cell lines (left panel) by slot-blotting, one ALT cell line (CHLA-90), and one telomerase-positive cell line (CHLA-136) are included as controls. Right panel, C-circle assay in COG-N-518x and COG-N-649x PDXs, one ALT PDX (COG-N-589x) and one telomerase positive PDX (Felix-PDX) are included as controls. (E) TRAP assay on the same neuroblastoma cell lines and PDXs as shown in D. (F) Terminal restriction fragment (TRF) length analysis to determine telomere length in LA-N-6, COG-N-291, CHLA-132, COG-N-509hnb, and COG-N-562hnb Cell lines. Control DNA was from two ALT cell lines (CHLA-90 and SK-N-FI) and two telomerase-positive cell lines (SK-N-BE(2) and CHLA-136). (G) Telomere and centromere FISH in COG-N-518x and COG-N-649x. One ALT-positive PDX (COG-N-589x) and one telomerase-positive PDX (Felix-PDX) are used as controls. The graph below represents telomere/centromere ratio per individual cell (measured in a minimum of 30 individual cells per PDX) in the PDXs above. ***: $P < 0.001$, ****: $P < 0.0001$. *P*-value was by Wilcoxon rank-sum test.

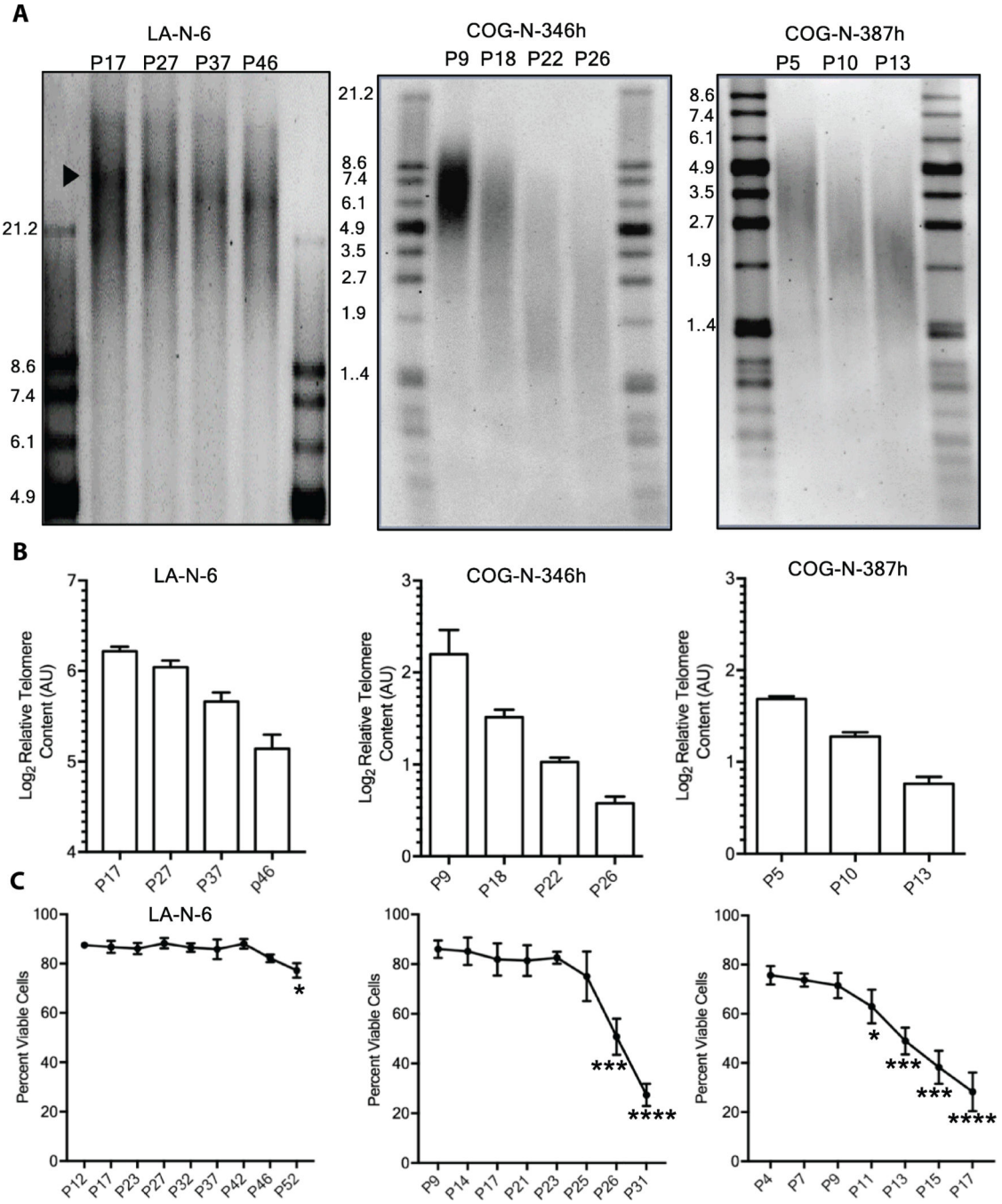

Figure. 5. TERT-low and ALT-negative NB cell lines established from high-risk neuroblastoma patients continuously shorten their telomeres.

(A) Terminal restriction fragment (TRF) length analysis of telomerase-low and ALT-negative NB cell lines LA-N-6 (with telomere content (TC) >5; non-*MYCN*-Amp), COG-N-346h (TC<5; non-*MYCN*-Amp), and COG-N-387h (TC<5; *MYCN*-Amp) shows telomere length shortening with progressive passage in culture. (B) Total telomere content measure by qPCR in the same cell lines as above during progressive passage in culture. (C)

Viability of the same cell lines as above during progressive passages in culture. *: $P < 0.05$, ***: $P < 0.001$, ****: $P < 0.0001$. P-value was determined using two-tailed Student t test.

Table 1.

Patient characteristics of neuroblastoma patients at diagnosis based on risk stratification.

Characteristic	Risk groups				All Patients	
	High Risk (n=110)		Low/Intermediate Risk (n=24)			
Age at Diagnosis	**N**	**Percent**	**n**	**Percent**	**n**	**Percent**
< 18 months	3	3%	24	100%	27	20%
>= 18 months	107	97%	0	0%	107	80%
Gender						
Male	64	58%	18	75%	82	61%
Female	46	42%	6	25%	52	39%
INSS stage						
2 or 3	1	1%	4	17%	5	4%
4	108	98%	1	4%	109	81%
4s	1	1%	19	79%	20	15%
***MYCN* Status**						
Not Amplified	79	72%	24	100%	103	77%
Amplified	30	27%	0	0%	30	22%
Unknown	1	1%	0	0%	1	1%
Histology						
Favorable	3	3%	22	92%	25	19%
Unfavorable	99	90%	1	4%	100	75%
Unknown	8	7%	1	4%	9	7%
Ploidy						
Hyperdiploid	54	49%	20	83%	74	55%
Diploid	55	50%	4	17%	59	44%
Unknown	1	1%	0	0%	1	1%
Grade						
Differentiating	7	6%	0	0%	7	5%
Undifferentiated or Poorly Differentiated	86	78%	23	96%	109	81%
Unknown	17	15%	1	4%	18	13%

Table 2.

EFS and OS probability estimates at 1 to 10 years from diagnosis in TERT-H, ALT, and TERT-L/non-ALT groups.

Time	TERT-H				ALT				TERT-L & non-ALT			
	EFS		OS		EFS		OS		EFS		OS	
	Estimate	SE	Estimate	SE	Estimate	SE	Estimate	SE	Estimate	SE	Estimate	SE
1 Year	0.758	0.059	0.831	0.051	0.840	0.073	0.960	0.039	0.821	0.072	1.000	0.000
2 Years	0.370	0.067	0.657	0.066	0.709	0.093	0.918	0.055	0.536	0.094	0.929	0.049
3 Years	0.292	0.063	0.439	0.069	0.488	0.104	0.743	0.091	0.464	0.094	0.857	0.058
4 Years	0.253	0.060	0.359	0.067	0.443	0.104	0.609	0.102	0.429	0.094	0.784	0.078
5 Years	0.233	0.059	0.279	0.063	0.287	0.099	0.469	0.106	0.429	0.094	0.747	0.083
6 Years	0.233	0.059	0.279	0.063	0.287	0.099	0.353	0.107	0.390	0.093	0.747	0.083
7 Years	0.195	0.061	0.279	0.063	0.287	0.099	0.236	0.120	0.390	0.093	0.747	0.083
8 Years	0.195	0.061	0.223	0.071	0.287	0.099	0.236	0.120	0.390	0.093	0.747	0.083
9 Years	0.195	0.061	0.223	0.071	0.287	0.099	0.236	0.120	0.390	0.093	0.747	0.083
10 Years	0.195	0.061	0.223	0.071	0.287	0.099	0.236	0.120	0.390	0.093	0.747	0.083